Regular Article

PHYSICAL CHEMISTRY RESEARCH
Published by the
Iranian Chemical Society
www.physchemres.org
info@physchemres.org

***Phys. Chem. Res.**, Vol. 6, No. 4, 825-838, December 2018*
DOI: 10.22036/pcr.2018.140584.1507

Molecular Dynamics Simulation of Crocin and Dimethylcrocetin Interactions with DNA

E. Azarhazin, M. Izadyar* and M.R. Housaindokht

Computational Chemistry Research Lab., Department of Chemistry, Faculty of Science, Ferdowsi University of Mashhad, Mashhad, Iran

(Received 13 July 2018, Accepted 5 October 2018)

In this work, the interactions of the crocin and dimethylcrocetin (DMC) as anti-cancer drugs with the Dickerson DNA model was investigated. Molecular dynamic simulations of Crocin, DMC and DNA composed of twelve base pairs and a sequence of the $d(CGCGAATTCGCG)_2$ were executed for 25 ns in water. Binding energy analysis for each of the complexes in three definite parts of B-DNA showed that Van der Waals interactions have a dominant contribution in energy values. Crocin-DNA interactions are greater than those of DMC-DNA, due to a longer Π-conjugation. The most probable interactions were detected by Gibbs energy analysis, indicating that the stabilizing interactions of the DNA with crocin and DMC are located in the major and minor grooves of the DNA, respectively. In the case of DMC, the binding energy of the A-T rich sequence is more than that of G-C which is different from crocin. Radial distribution function analysis showed that two sharp peaks of the CO…NH and HO…OC parts, during the complex formation at 2.16 Å and 2.28 Å, could be assinged to the new hydrogen bond formation between DMC and crocin with DNA, respectively. Also, non-classical H-bonds were investigated by considering the CH group of the drug and OC/NC groups of DNA that play an important role in the stability of the DNA in the corresponding complex.

Keywords: Crocin, Dimethylcrocetin, Molecular dynamic, H-bond, Dickerson, Force field, DNA

INTRODUCTION

The biological role of the natural products has been widely proven in declining the risk of cancer and delaying carcinogenesis on the human and animal models [1-5]. Today, there is a great interest to examine the role of different plant species and their derivatives in reducing tumor formation [4,6]. Saffron and its related carotenoids have been widely used in recent years because of their biomedical properties, especially as anticancer [7-13]. Experiments show the effect of saffron and its main ingredients on the treatment of several types of cancer [7].

Using experimental techniques, volatile and bitter compounds such as safranal and carotenoid derivatives of crocetin have been identified in the saffron dried stigma, having the pharmacological effects [14]. The most important parts of the saffron stigma are carotenoids of crocetin and crocin [15,16], which are inhibitors for the cancer cells [17] and free radicals [18-20]. Findings on the crocin and dimethylcrocetin effects in the biosynthesis of DNA and RNA, using DNA marker derived from Leukemia P388 cells indicate that both compounds suppress the synthesis of DNA and RNA [21].

In 2011, Perveen *et al.* reported the results of a joint experimental and theoretical study on the antheracycline anti-cancer drugs, such as doxorubicin, dctinomycin, daunorubicin, epirubicin and mitoxantrone [22]. The docking results were analyzed and compared with experimental data to understand the nature of these interactions with DNA. Also, the stability of drug-DNA complexes was discussed through the intercalation and groove binding mechanisms.

In 2014, Sarwar and colleagues studied esculetin interactions with calf thymus DNA as an anti-cancer [23].

*Corresponding author. E-mail: izadyar@um.ac.ir

They investigated the binding mode of the drug-DNA complex using various spectroscopic techniques, melting point and viscosity measurements, and thermodynamic parameters calculations. These analyses showed that hydrophobic interactions and hydrogen bonds are the driving force of the binding process. They also claimed that esculetin interacts with the minor groove of ct-DNA.

In 2007, Bathaie et al. investigated the interaction of the saffron carotenoids with ct-DNA using the spectroscopic techniques [24]. The obtained results confirmed the non-intercalative carotenoids coupling to a small groove, without binding restriction to the GC or AT sequence.

In 2017, Silva group studied the interaction of anti-cancers of pterocarpan with ct-DNA using the molecular docking, molecular dynamic and experimental methods [25]. On the basis of different analyses, they proposed that the interaction of hydrophobic compounds in the DNA groove plays an important role in coupling.

Accordingly, to discover some parts of the unknown mechanism aspects of the drug-DNA interaction, this research was performed on the crocin-DNA and DMC-DNA complexes using a MD simulation approach. Moreover, a knowledge of the interaction mechanism is of great importance to design new efficient drugs in cancer treatment

Although several hypotheses have been developed to determine the mechanism of action of the saffron based on the carotenoid activity, the molecular aspects of anti-cancer and anti-tumor effects of the saffron and its derivatives are unknown. Therefore, more precise studies are needed to control carcinogenesis using the modified drugs obtained from these compounds [26].

Due to some disadvantages of available analytical techniques to study the interactions of DNA with small drug molecules, such as high cost and low sensitivity [27,28], analyzing the intermediate structures by the molecular dynamic simulations could be a practical way to increase our understanding of the drug properties and the mechanism under which drug molecules interact with DNA [29-31].

Molecular Dynamic Simulation Details

All MD simulations were accomplished in water utilizing the Amber 14.0 software package [32]. Amber force field of ff14SB [33] and general Amber force fields (GAFF) [34] were employed for DNA and drugs, respectively. Chemical structure of the crocin and dimethylcrocetin, Fig. 1, was optimized, at B3LYP/6-31G (d,p) level [35,36], using the G09 computational package [37].

The initial skeleton of B-DNA was created by the Abalone software [38]. B-DNA is a right-handed double-stranded helix of DNA that was determined first by Watson and Crick [39]. This form of DNA is the most common DNA helix conformation under physiological conditions [40]. After designing the B-DNA, total charge neutrality was achieved by addition of 50 cations of Na^+. Mass unrestraint (non-rigidity) and the solvated model of the compound-DNA were achieved in the presence of 11075 to 15111 water molecules within TIP3P potential for the simulation of water, in which three-site model has three interaction points corresponding to the three atoms of water molecule. These potential functions supply a logical description of the liquid water that is useful in the simulation of chemical systems of water [41]. Each site has a point charge, and the corresponding site to the oxygen atom also has the Lennard-Jones parameters. Since three-site models produce a high computational efficiency, they are widely used in MD simulations [41,42].

Energy minimization of drug-DNA complexes was implemented in 40000 cycles. Then, each structure was heated in an NVT ensemble from 0 to 300 K for 2000 ps. All simulations on the complexes were performed in three regions (S1, S2 and S3), as shown in Fig. 2. On the basis of the obtained data, minimization energies related to S1, S2 and S3 for crocin, are -281.83, -260.33, -260.98 kcal mol^{-1} and -241.24, -324.21, -300.744 kcal mol^{-1}, for dimethylcrocetin, respectively.

The obtained data for each complex were used as input for the equilibration step, during the 1000 ps in an NPT ensemble (300 K and 1 bar). MD simulations of the products were done for 25 ns in an NPT ensemble using a 1fs time step. Periodic boundary conditions, using Ewald summation [43,44], were used for calculating the long-range electrostatic interactions in 8 Å direct space cut off. Since Particle Mesh Ewald (PME) method offers several advantages, such as high accuracy, continuity and efficiency for the treatment of long-range forces in macromolecular systems [45], this method coupled with the periodic

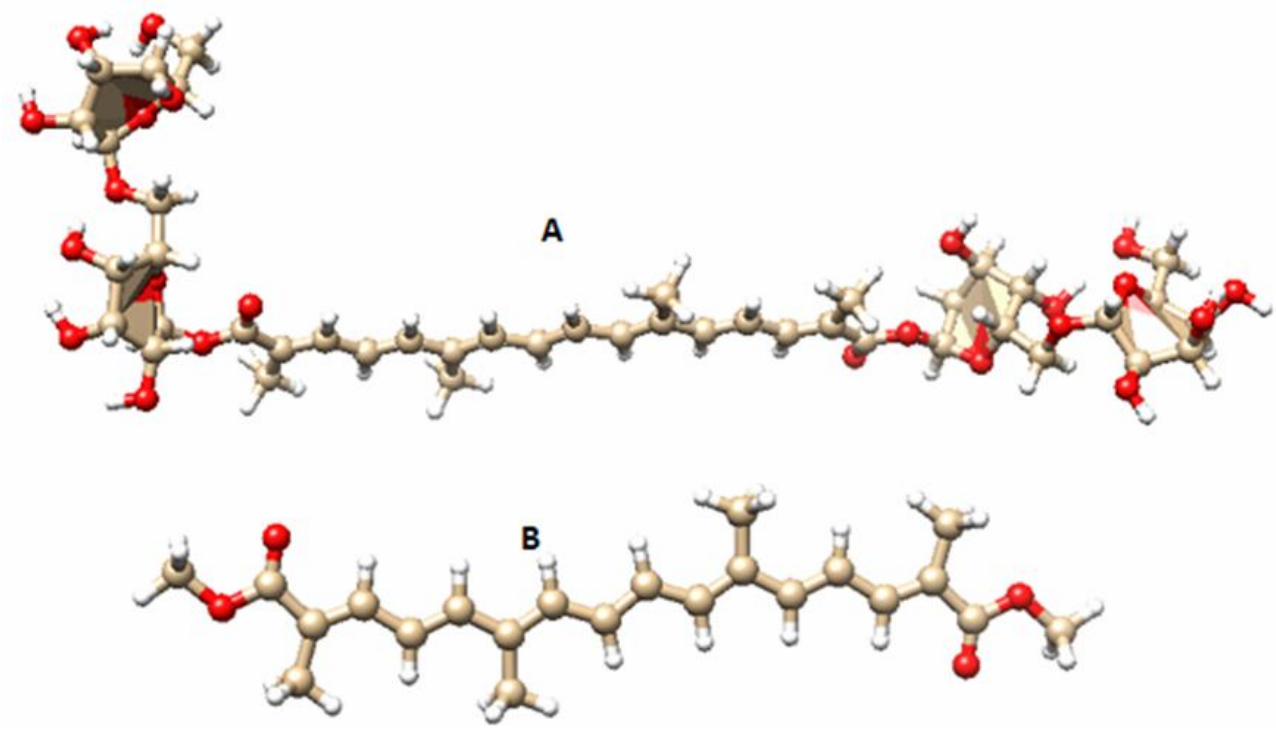

Fig. 1. Optimized structures of crocin (A) and dimethylcrocetin (B) at B3LYP/6-31G (d,p) level of theory; H, O and C atoms are in white, red and blue colors, respectively.

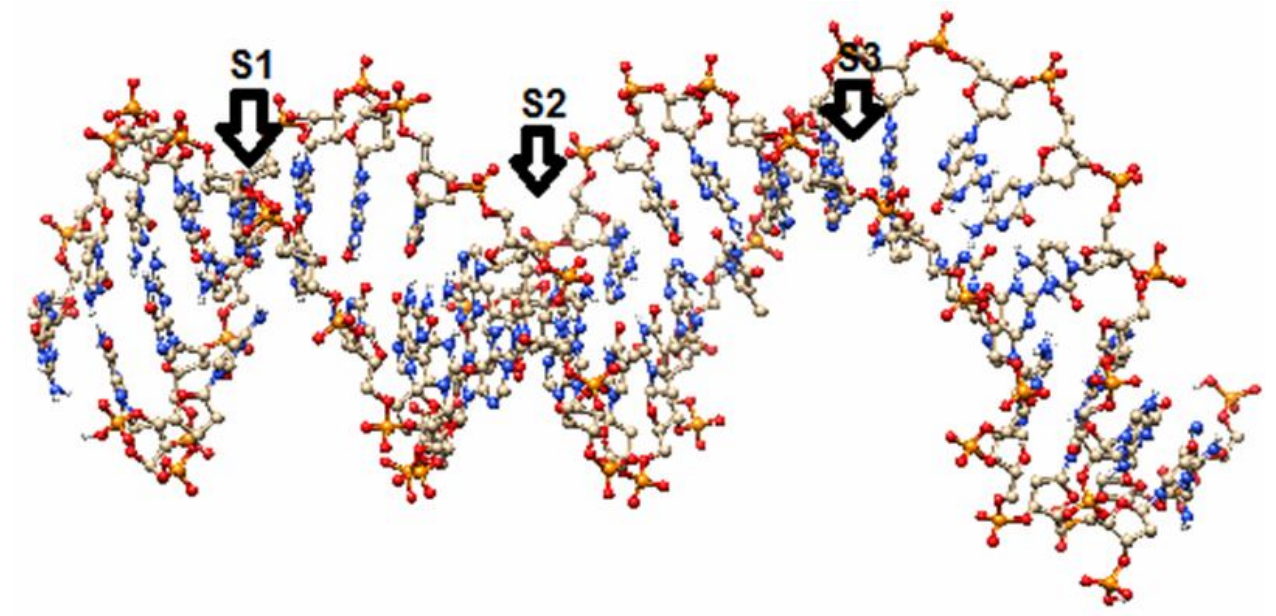

Fig. 2. Three definite regions of B-DNA, named as S1, S2 and S3 after 25 ns simulation.

boundary conditions was used for calculating the long-range electrostatic interactions. To control the temperature of the systems with a collision frequency of 2 ps^{-1} and a pressure relaxation time of 2 ps in an NPT ensemble, Langevin thermostat was used [46,47].

Gibbs energy of binding for each 1:1 drug-DNA complex was calculated, using the molecular mechanics generalized-Born surface area (MM-GBSA) method as performed in Amber Tools 13.0 [48-50]. In this method, molecular mechanics energies combined with the Poisson-Boltzmann or Generalized Born50 and surface area continuum solvation methods have been employed to estimate the interaction energy and correlation coefficients of small ligands binding to biological macromolecules [51,52]. Harmonic approximation of translational, rotational and vibrational conformational entropies were applied by the normal mode analysis program of the MM-PBSA package [50-53]. In MM/PBSA or MM/GBSA, binding free energy (ΔG_{bind}) of the ligand-receptor in the complex is calculated using the Eq. (1) [54],

$$\Delta G_{bind} = \Delta E_{MM} + \Delta G_{sol} - T\Delta S \quad (1)$$

where ΔE_{MM} is the changes of the gas phase MM energy, ΔG_{sol} is the solvation Gibbs energy, and in the final TS term, T is the absolute temperature and S is the entropy obtained by normal mode analysis of the vibrational frequencies. ΔE_{MM} is obtained using Eq. (2),

$$\Delta E_{MM} = \Delta E_{internal} + \Delta E_{electrostatic} + \Delta E_{vdw} \quad (2)$$

where $E_{internal}$, $E_{electrostatic}$ and E_{vdw} are the internal energy terms obtained from the bonded, electrostatic and van der Waals interactions, respectively. Solvation Gibbs energy is calculated according to Eq. (3),

$$\Delta G_{sol} = \Delta G_{Pol} + \Delta G_{np} \quad (3)$$

where ΔG_{pol} and ΔG_{np} are the polar and nonpolar contributions of the solvation free energy, respectively. Nonpolar contribution of the solvation free energy was calculated by nonpolar solvation term based on the solvent-accessible surface area (SASA) [55]. The nonpolar contribution to the solvation free energy is related to cavity formation and van der Waals interactions between the solute and the solvent, in which solvent-accessible surface area is directly correlated with $\Delta G_{np.}$ according to Eq. (4) [55],

$$\Delta G_{np} = \gamma\ SASA + b \quad (4)$$

where γ is the surface tension proportionality constant and b is a constant.

RESULTS AND DISCUSSION

Molecular dynamic simulations of the considered structures (DNA, crocin-DNA, DMC-DNA) in water were carried out for 25 ns. Theoretical calculations were performed on a nanostructure model of DNA, consisting of twelve base pairs, $d[CGCGAATTCGCG]_2$ and 40 Å in length. This part of DNA is known as the Dickerson dodecamer that has been already considered as a DNA model [56].

In all MD simulations, three specific regions of B-DNA, S1, S2 and S3 were considered as the most probable interaction sites from the thermodynamic point of view (Fig. 2). According to Fig. 2, it is confirmed that the chosen regions are in the minor (S1, S3) and major S2 grooves of the B-DNA.

To investigate the structural stability of DNA, crocin-DNA and DMC-DNA complexes, root mean square deviation (RMSD) values for the heavy atoms of C, N and P of DNA and complexes were calculated in water, during the 25 ns MD simulation (Figs. 3A and 4A). This analysis is a measure of average distance between the atoms, usually the backbone atoms of the superimposed macromolecules [57]. These calculations were performed on the initial geometries obtained from the MD trajectory as shown in Figs. 3 and 4. Based on the values reported in these figures, the degrees of fluctuation are low during the simulation, demonstrating a suitable stability of the DNA, crocin-DNA and DMC-DNA complexes in water (Figs. 3A, 4A). The stability was confirmed by the radii of gyration (Rg) analysis for the drug-DNA complex (Figs. 3B and 4B). Maximum RMSD values of DNA, crocin-DNA and DMC-DNA complexes are 0.41, 0.77, 0.99 nm, respectively. According to the higher RMSD values, DMC-DNA complex is less stable than crocin-DNA in water, due to polar solvent effects on

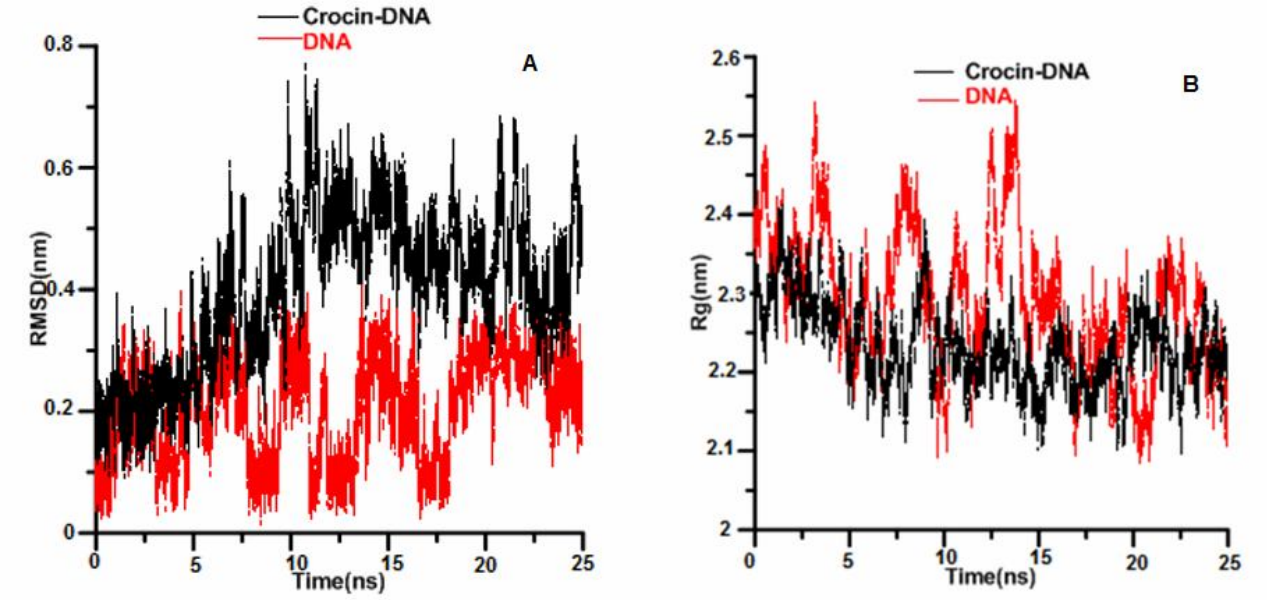

Fig. 3. Calculated RMSD (A) and Rg (B) values of crocin-DNA and DNA as a function of time during 25 ns at S2 region.

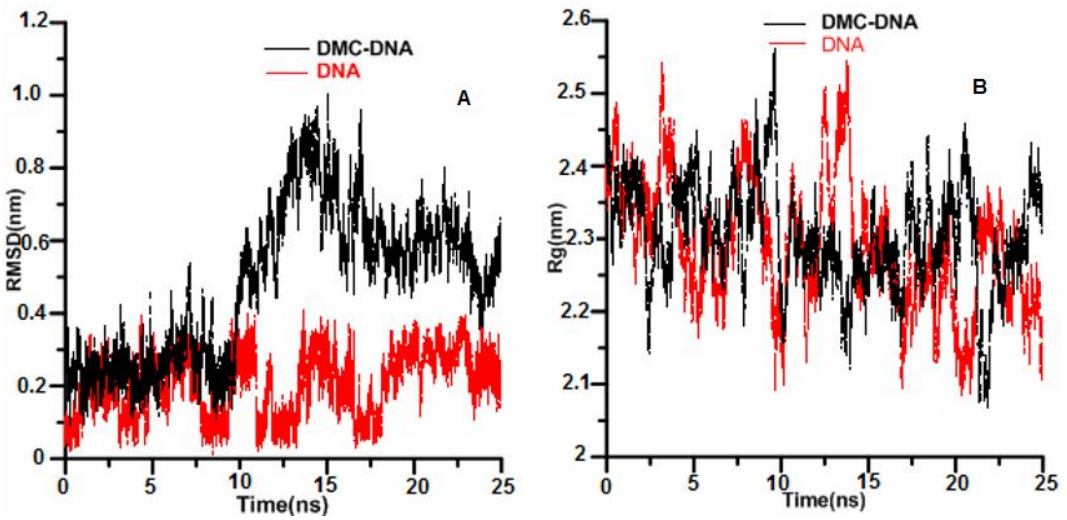

Fig. 4. Calculated RMSD (A) and Rg (B) values of DMC-DNA and DNA as a function of time, during 25 ns at S3 region.

the polar groups of the drug. This means that dipole moments of crocin and DMC are 15.03D and 0.16 D, respectively, confirming a higher stability of the drug in crocin-complex in polar solvent such as water, in comparison with DMC-DNA. Rg analysis of the DNA and each complex was done in water.

Maximum Rg values of DNA, crocin-DNA and DMC-DNA are 2.55, 2.42, 2.56 (nm), respectively, indicating that the distance between different units of the DMC-DNA complex is higher than that of crocin-DNA in water. A

Table 1. Calculated Total Gibbs Energy of Binding and Entropy at Different Regions of Crocin-DNA and DMC-DNA Complexes by GB Method

Complex	Parameter	Region	Average value	Standard deviation	Standard error of mean
	ΔG	S_1	-24.1	2.94	0.42
	(kcal mol^{-1})	S_2	-64.6	2.80	0.40
		S_3	-44.9	2.90	0.40
crocin-DNA					
	ΔS	S_1	-32.6	1.06	0.33
	(cal mol^{-1} K^{-1})	S_2	-45.1	1.31	0.41
		S_3	-35.2	0.77	0.24
	ΔG	S_1	-25.2	1.63	0.23
	(kcal mol^{-1})	S_2	-30.4	2.07	0.29
		S_3	-33.1	2.44	0.35
DMC-DNA					
	ΔS	S_1	-26.8	1.78	0.56
	(cal mol^{-1} K^{-1})	S_2	-29.6	1.35	0.43
		S_3	-22.5	2.76	0.88

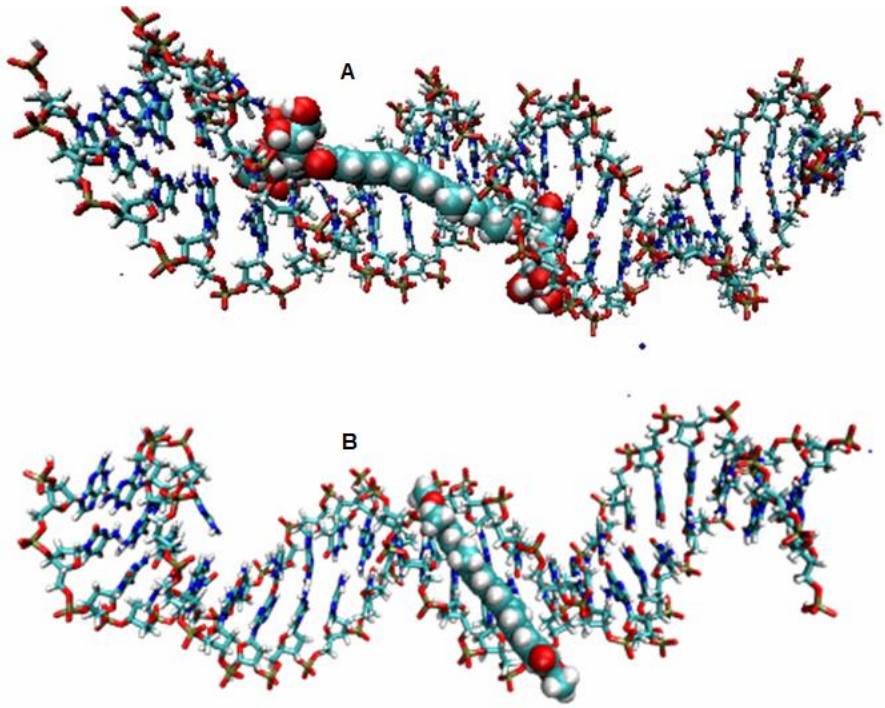

Fig. 5. The snapshot of crocin-DNA interactions at the major groove of S2, (A) and DMC-DNA interactions at the minor groove of S3, during the 25 ns MD simulation.

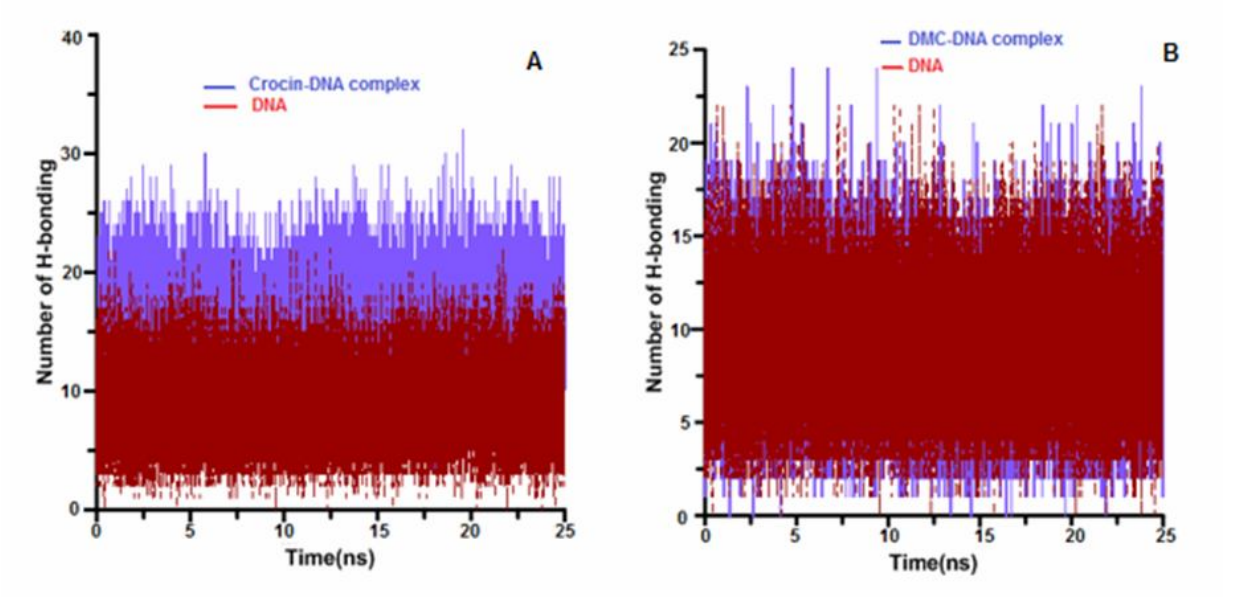

Fig. 6. H-bonding analysis of the isolated DNA and crocin-DNA (A) and DMC-DNA (B) complexes during the 25 ns simulation.

greater value of Rg demonstrates that the complex structure is less compact.

A major disadvantage of using the PB method in comparison with GB is low precision, (Low standard deviation) [58,59], therefore Gibbs energies and entropies were calculated using the GB method and are reported in Table 1. Stabilizing interactions, obtained by ΔG calculations, demonstrated that maximum and minimum interactions for crocin-DNA complex are related to S2 and S1 regions, respectively, and the corresponding values are -64.6, -24.1 kcal mol^{-1}, in these regions. In the case of DMC-DNA complex, interaction energies are -33.1, -25.2 kcal mol^{-1} concerning to the S3 and S1 regions, respectively. This means that the most probable interaction sites of DNA with crocin and DMC are located in the major and minor grooves of DNA, respectively. Since crocin is almost a large molecule, further interactions occur in the major groove of DNA. Figure 5 shows the equilibrated drug-DNA structure after 25 ns MD simulation. All snapshots of the configurations were obtained using the VMD package [60].

Moreover, on the basis of trajectory analysis of the drug in the mediocre sequence of DNA (Fig. 5) and Gibbs energy values, calculated at different regions, it is verified that in the case of DMC complex, the binding energy of the A-T rich sequence is more than that of G-C sector. Therefore, DMC binds to the AT-rich region, similar to curcumin, lafutidine and crocetin drugs [61,62,31], while the most important interactions in crocin are related to A-T rich and C-G rich regions. Total entropies calculated verified the complexation process during the simulation time.

To investigate the effect of hydrogen bond on the stability of the DNA structure during the complexation, hydrogen bond analysis was performed. Figure 6 demonstrates the results of the H-bonding in the isolated DNA, crocin-DNA, and DMC-DNA complexes. According to the calculations, average hydrogen bond number in the isolated DNA and DNA in the crocin-DNA, DMC-DNA complexes is 8.84, 8.72 and 8.67, respectively. This means that the interaction of DMC with DNA decreases the stability of the DNA structure, while the average number of H-bonding of the crocin-DNA and DMC-DNA is 14.42, 8.67, respectively. These results totally make sense, because in the case of crocin-DNA, RMSD and Rg values are lower due to a higher number of hydrogen bonding. On the basis of results calculated, the number of H-bonds in the complex increases in comparison with the isolated DNA, therefore the complex structure of the DMC-DNA is less stable. On

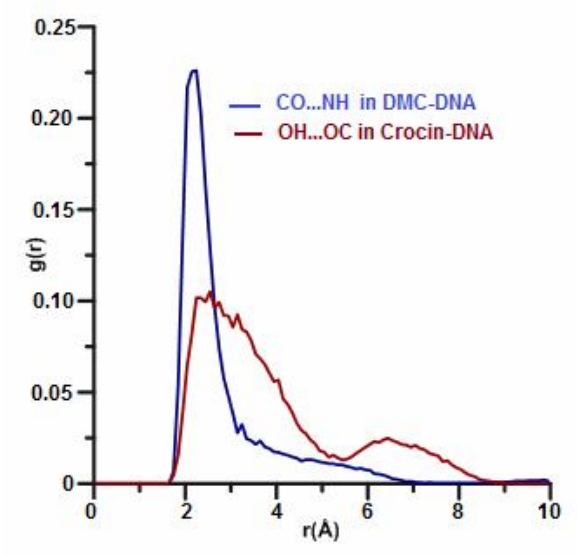

Fig. 7. RDF diagrams of the NH group of DNA with the CO group of the DMC and CO and OC groups of DNA with the OH group of crocin after 25 ns MD simulation.

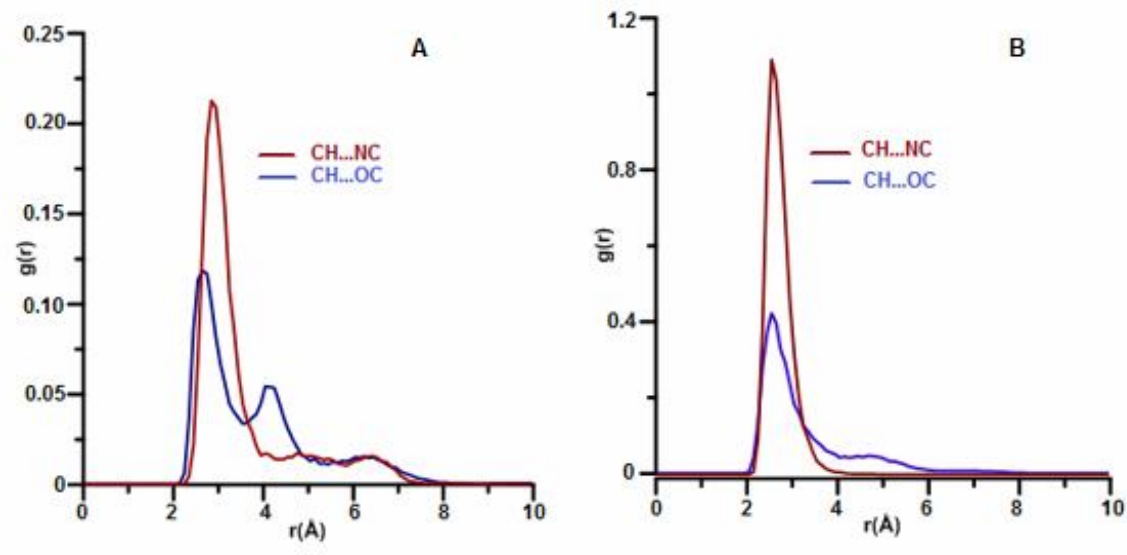

Fig. 8. RDF diagrams of the NC and OC groups of the DNA with the CH group of DMC (A) and the CO and NC groups of DNA with the CH group of crocin (B) after 25 ns MD simulation.

the basis of Al-Otaibi and coworkers' studies, crocin acts an anticancer compound, because the number of hydrogen bonds of the interaction site with DNA is greater.[63] Obtained MD data are in good agreement with the IC_{50} values reported in experimental studies [64].

Figure 7 indicates the radial distribution functions (RDF) of the CO…NH and HO…OC parts during the complex formation. Two sharp peaks at 2.16 Å and 2.28 Å are related to the new hydrogen bond formation between DMC and crocin with DNA, respectivily. Also, non-

Table 2. Binding Energy Ingredients (kcal mol^{-1}) Calculated by GB Method, During the 25ns MD Simulation

Complex	Parameter	Average value			Standard deviation			Standard error of mean		
		S1	S2	S3	S1	S2	S3	S1	S2	S3
Crocin-DNA	ΔE_{vdw}	-69.8	-82.2	76.1	2.92	2.64	2.51	0.41	0.37	0.35
	ΔE_{ele}	-11.3	-13.4	-13.7	9.83	4.63	7.70	1.39	0.65	1.08
	ΔE_{GB}	23.5	41.0	52.7	9.61	4.71	8.10	1.36	0.67	1.14
	ΔE_{surf}	-7.01	-10.0	-7.8	0.22	0.28	0.24	0.03	0.04	0.03
	ΔG_{gas}	-58.6	-95.6	-89.8	10.19	5.92	8.15	1.44	0.84	1.15
	ΔG_{sol}	16.5	31.1	45.0	9.59	4.65	8.02	1.36	0.66	1.13
DMC-DNA	ΔE_{vdw}	-30.5	-35.6	48.9	1.76	2.04	2.29	0.25	0.29	0.32
	ΔE_{ele}	0.7	1.2	2.9	0.97	0.68	1.99	0.14	0.10	0.28
	ΔE_{GB}	9.0	9.1	18.0	0.74	0.72	2.14	0.19	0.10	0.30
	ΔE_{surf}	-4.4	-5.1	-5.1	0.23	0.20	0.15	0.03	0.03	0.02
	ΔG_{gas}	-29.8	-34.4	-46.0	1.84	2.09	2.87	0.26	0.29	0.41
	ΔG_{sol}	4.6	4.0	12.8	0.66	0.64	2.07	0.09	0.09	0.29

classical H-bonds of CH…OC and CH…NC were analyzed as shown in Fig. 8. This type of H-bond was reported, previously [65,66]. Two sharp peaks at 2.65 Å and 2.85 Å, and also two sharp peaks at 2.54 Å are related to the unusuall intermolecular H-bond interactions between DMC and crocin with DNA that play an important role in the stability of DNA in the complex.

Different parts of binding energy for two complexes were calculated using the GB method, and are reported in Table 2. Comparison between the different contributions of the binding energy shows the dominant performance of van der Waals interactions. The interaction value for crocin is greater than that for DMC, and the most important interactions are related to the phenyl ring and the reciprocal O, N and H atoms between the crocin and DNA, during the 25 ns MD simulation. Polar solvents such as water have the highest hydrophilic interaction with the isolated components and complex leading to reduce the electrostatic energy. Therefore, the anticancer effect of the both drugs can be correlated with the van der Waals and hydrogen bonding interactions that are greater in the case of crocin.

CONCLUSIONS

In this research, molecular dynamic simulations were used to investigate the interaction of crocin and DMC with the B-DNA model. The 25 ns MD simulations of the complexes in water show that the crocin-DNA complex is more stable in water than DMC-DNA, because of the great value of RMSD in water in the major groove of DNA. Rg analysis shows that theoretical distance between the different units of the complexes in DMC-DNA is lower than that of crocin-DNA, because a larger Rg value demonstrates that the complex structure is lees compact. Trajectory analysis of the compound in the mediocre, and Gibbs energy values calculated at different regions verify that the binding energy of the A-T rich sequence is more than that of

the G-C sector in DMC. Therefore, DMC binds to the AT-rich region, similar to curcumin, lafutidine and crocetin. The most important interactions in the crocin are from one side to the A-T rich region, and from the other side to the G-C rich region. Calculated total entropies verified the complexation process during the simulation time. H-bond analysis shows an improvement in the number of H-bonds in the crocin-DNA complex relative to the isolated DNA, therefore the complex structure of the crocin-DNA is more stable. It is reasonable to conclude that crocin acts an anticancer drug because the number of hydrogen bonds is greater. The obtained MD data are in good agreement with the IC_{50} results in the experimental studies. Finally, on the basis of different analyses, a correlation between the anti-cancer effects of these drugs and hydrogen bond interactions is predictable.

ACKNOWLEDGEMENTS

Research council of Ferdowsi University of Mashhad is acknowledged for financial supports (Grant No. 3/38552). Also, the authors claimed that there is not any conflict of interest.

REFERENCES

[1] Steele, V. E.; Lubet, R. A., The use of animal models for cancer chemoprevention drug development. *Semin. Oncol.* **2010**, *37*, 327-38. DOI: 10.1053/ j.seminoncol.2010.05.010.

[2] Nijhoff, W. A.; Groen, G. M.; Peters, W. H. M., Induction of rat hepatic and intestinal glutathione S-transferases and glutathione by dietary naturally occurring anticarcinogens. *Int. J. Oncl.* **1993**, *3*, 1131-1139. DOI: 10.3892/ijo.3.6.1131.

[3] Campbell, T. C., Nutrition and cancer: an historical perspective. 1. Was a nutritional association acknowledged a century ago? *Nutr. Cancer.* **2017**, *8*, 1-7. DOI: 10.1080/01635581.2017.1317823.

[4] Conney, A. H.; Lysz, T.; Ferraro, T.; Abidi, T. F.; Manchand, P. S.; Laskin, J. D.; Huang, M. T., Inhibitory effect of curcumin and some related dietary compounds on tumor promotion and arachidonic acid metabolism in mouse skin. *Adv. Enzyme Regul.* **1991**, *31*, 385-391. DOI: 10.1016/0065-2571(91)90025-H.

[5] Wallace, T. C.; Murray, R.; Zelman, K. M., The Nutritional Value and Health Benefits of Chickpeas and Hummus. *Nutrients*. **2016**, *8*, 766-776. DOI: 10.3390/nu8120766.

[6] Polasa, K.; Sesikaran, B.; Krishna, T. P.; Krishnasway, K., Turmeric-induced reduction in urinar mutagens. *Food Chem. Toxicol.* **1991**, *29*, 699-706. DOI: 10.1016/0278-6915(91)90128-T.

[7] Saeed Samarghandian, S.; Abasalt Borji, A., Anticarcinogenic effect of saffron (Crocus sativus L.) and its ingredients. *Pharmacognosy. Res.* **2014**, *6*, 99-107. DOI: 10.4103/0974-8490.128963

[8] Abdullaev, F. I.; Espinosa-Aguirre, J. J., Biomedical properties of saffron and its potential use in cancer therapy and chemoprevention trials. *Cancer Detect. Prev.* **2004**, *28*, 426-432. DOI: 10.1016/ j.cdp.2004.09.002.

[9] Pitsikas, N., Constituents of saffron (crocus sativus L.) as potential candidates for the treatment of anxiety disorders and schizophrenia. *Molecules*. **2016**, *21*, 303-404. DOI: 10.3390/ molecules21030303.

[10] Abdullaev, F. I. Riverón-Negrete, L.; Caballero-Ortega, H.; Manuel Hernández, J.; Pérez-López, I.; Pereda-Miranda, R.; Espinosa-Aguirre, J. J., Use of *in vitro* assays to assess the potential genotoxic and cytotoxic effects of saffron (Crocus sativus L.). *Toxicol. In. Vitro*. **2003**, *17*, 731-736. DOI: 10.1016/ S0887-2333(03)00098-5.

[11] Srivastava, R.; Ahmed, H.; Dixit, R. K.; Dharamveer, Saraf, S. A., Crocus sativus L.: A comprehensive review. *Pharmacogn. Rev.* **2010**, *4*, 200-208. DOI: 10.4103/0973-7847.70919.

[12] Zheng, C. J.; Li, L.; Ma, W. H.; Han, T.; Qin, L., Chemical constituents and bioactivities of the liposoluble fraction from different medicinal parts of Crocus sativus. *Pharm. Biol.* **2011**, *49*, 756-63. DOI: 10.3109/13880209.2010.547206.

[13] Zareena, A. V.; Variar, P. S.; Chlar, A. S.; Bongirwar, D. R., Chemical investigation of g-irradiated saffron (Crocus sativus L.). *J. Agric. Food Chem.* **2001**, *49*, 687-691. DOI: 10.1021/jf000922l.

[14] Sampathu, S. R.; Shivashankar, S.; Lewis, Y. S., Saffron (Crocus sativus L.). Cultivation, processing,

chemistry and standardization. *CRC Crit. Rev. Food Sci. Nutr.* **1984**, *20*, 123-157. DOI: 10.1080/10408398409527386.

[15] Giaccio, M., Crocetin from Saffron: An Active Component of an Ancient Spice. *Crit. Rev. Food Sci. Nutr.* **2004**, *44*, 155-72. DOI: 10.1080/10408690490441433.

[16] Alavizadeh, S. H.; Hosseinzadeh, H., Bioactivity assessment and toxicity of crocin: A comprehensive review. *Food Chem. Toxicol.* **2014**, *64*, 65-80. DOI: 10.1016/j.fct.2013.11.016.

[17] Bolhassani, A.; Afshin Khavari, A.; Zahra Bathaie, S. Z., Saffron and natural carotenoids: Biochemical activities and anti-tumor effects. *Biochim. Biophys. Acta.* **2014**, *1845*, 20-30. DOI: 10.1016/j.bbcan.2013.11.001.

[18] Abe, K.; Saito, H., Effects of saffron extract and its constituent crocin on learning behaviour and long-term potentiation. *Phytother. Res.* **2000**, *14*, 149-152. DOI: 10.1002/(SICI)1099-1573(200005).

[19] Zhang, Z.; Wang, C.; Wen, X.; Shoyama, Y.; Yan, C., Role of saffron and its constituents on cancer chemoprevention. *Pharm. Biol.* **2013**, *51*, 920-924, DOI: 10.3109/13880209.2013.771190

[20] Erben-Russ, M.; Michel, C.; Bors, W.; Saran, M., Determination of sulfite radical reaction rate constants by means of competition kinetics. *Radiat. Environ. Biophys.* **1987**, *26*, 289-294. DOI: 10.1007/BF01221974.

[21] Nair, S. C.; Panikkar, B.; Panikker, K. R., Antitumor activity of Saffron. *Cancer Lett.* **1991**, *57*, 109-114. DOI: 10.1016/0304-3835(91)90203-T.

[22] Perveen, F.; Qureshi, R.; Ansari, F. L.; Kalsoom, S.; Ahmed, S., Investigations of drug-DNA interactions using molecular docking, cyclic voltammetry and UV-Vis spectroscopy. *J. Mol. Struct.* **2011**, *1004*, 67-73. DOI: 10.1016/j.molstruc.2011.07.027.

[23] Sarwar, T.; Husain, M. A.; Rehman, S. U.; Ishqi, H. M.; Tabish, M., Multi-spectroscopic and molecular modelling studies on the interaction of esculetin with calf thymus DNA. *Mol. Biosyst.* **2015**, *11*, 522-531. DOI: 10.1039/c4mb00636d.

[24] Bathaie, S. Z.; Bolhasani, A.; Hoshyar, R.; Ranjbar, B.; Sabouni, F.; Moosavi-Movahedi, A. A., Interaction of saffron carotenoids as anticancer compounds with ctDNA, Oligo (dG.dC)15, and Oligo (dA.dT)15. *DNA Cell Biol.* **2007**, *26*, 533 540. DOI: 10.1089/dna.2007.0598.

[25] Silvaa, M. M.; Nascimentoa, E. O. O.; Silva Júniora, E. F.; Araújo Júniora, J. X.; Santanab, C. C; Grillob, L. A. M.; Oliveirac, R. S.; Costad, P. R. R.; Buarquec, C. D.; Santos, J. C. C.; Figueiredoa, I. M., Interaction between bioactive compound11a-N-tosyl-5-deoxi-pterocarpan (LQB-223) and Calf thymus DNA:Spectroscopic approach, electrophoresis and theoretical studies. *Int. J. Biol. Macromol.* **2017**, *96*, 223-233. DOI: 10.1016/j.ijbiomac.2016.12.044.

[26] Stavric, B., Role of chemopreventers in human diet. *Clin. Biochem.* **1994**, *27*, 319-332. DOI: 10.1016/0009-9120(94)00039-5.

[27] Rauf, S.; Gooding, J. J.; Akhtar, K.; Ghauri, M. A.; Rahman, M.; Anwar, M. A.; Khalid, A. M., Electrochemical approach of anticancer drugs-DNA interaction. *J. Pharmaceut. Biomed.* **2005**, *37*, 205-217. DOI: 10.1016/j.jpba.2004.10.037.

[28] Cesconetto, E. C.; Junior, F. S. A.; Crisafuli, F. A. P.; Mesquita, O. N.; Ramosa, E. B.; Rocha, M. S., DNA interaction with Actinomycin D: mechanical measurements reveal the details of the binding data. *Phys. Chem. Chem. Phys.* **2013**, *15*, 11070-11077. DOI: 10.1039/C3CP50898F.

[29] Onodera, K.; Satou, K.; Hirota, H., Evaluations of molecular docking programs for virtual screening. *J. Chem. Inf. Model.* **2007**, *47*, 1609-1618. DOI: 10.1021/ci7000378.

[30] Verdonk, M. L.; Giangreco, I.; Hall, R. J.; Korb, O.; Mortenson, P. N.; Murray, C. W., Docking performance of fragments and druglike compounds. *J. Med. Chem.* **2011**, *54*, 5422-5431. DOI: 10.1021/jm200558u.

[31] Azarhazin, E.; Izadyar, M.; Housaindokht, M. R., Molecular dynamic simulation and DFT study on the Drug-DNA interaction; Crocetin as an anticancer and DNA nanostructure model. *J. Biomol. Struct. And Dynam.* **2018**, *36*, 1063-1074. DOI: 10.1080/07391102.2017.1310060.

[32] Case, D. A.; Babin, V.; Berryman, J. T.; Betz, R. M.; Cai, Q.; Cerutti, D. S.; Cheatham, III, T. E.; Darden,

T. A.; Duke, R. E.; Gohlke, H.; Goetz, A. W.; Gusarov, S.; Homeyer, N.; Janowski, P.; Kaus, J.; Kolossvary, I.; Kovalenko, A. F.; Lee, T. S.; LeGrand, S.; Luchko, T.; Luo, R.; Madej, B.; Merz, K. M.; Paesani, F.; Roe, D. R.; Roitberg, A.; Sagui, C.; Salomon-Ferrer, R.; Seabra, G.; Simmerling, C. L.; Smith, W.; Swails, J.; Walker, R. C.; Wang, J.; Wolf, R. M.; Wu, X.; Kollman, P. A., AMBER 14, University of California, San Francisco, 2014.

[33] Dickson, C. J.; Madej, B. D.; Skjevik, A. A.; Betz, R. M.; Teigen, K.; Gould, I. R.; Walker, R. C., Lipid14: The amber lipid force field. *J. Chem. Theory Comput.* **2014**, *10*, 865-879. DOI: 10.1021/ct4010307.

[34] Wang, J.; Wolf, R. M.; Caldwell, J. W.; Kollamn, P. A.; Case, D. A., Development and testing of a general amber force field. *J. Comput. Chem.* **2004**, *25*, 1157-1174. DOI: 10.1002/jcc.20035.

[35] Becke, A. D., Density-functional thermochemistry. III. The role of exact exchange. *J. Chem. Phys.* **1993**, *98*, 5648-5652. DOI: 10.1063/1.464913.

[36] Lee, C.; Yang, W.; Parr, R. G., Development of the Colle-Salvetti correlation-energy formula into a functional of the electron density. *Phys. Rev.* **1988**, *37*, 785-789. DOI: 10.1103/PhysRevB.37.785.

[37] Frisch, M. J.; Trucks, G. W.; Schlegel, H. B.; Scuseria, G. E.; Robb, M. A.; Cheeseman, J. R.; Montgomery, J. A., Jr.; Vreven, T.; Kudin, K. N.; Burant, J. C.; Millam, J. M.; Iyengar, S. S.; Tomasi, J.; Barone, V.; Mennucci, B.; Cossi, M.; Scalmani, G.; Rega, N.; Petersson, G. A.; Nakatsuji, H.; Hada, M.; Ehara, M.; Toyota, K.; Fukuda, R.; Hasegawa, J.; Ishida, M.; Nakajima, T.; Honda, Y.; Kitao, O.; Nakai, H.; Klene, M.; Li, X.; Knox, J. E.; Hratchian, H. P.; Cross, J. B.; Bakken, V.; Adamo, C.; Jaramillo, J.; Gomperts, R.; Stratmann, R. E.; Yazyev, O.; Austin, A. J.; Cammi, R.; Pomelli, C.; Ochterski, J. W.; Ayala, P. Y.; Morokuma, K.; Voth, G. A.; Salvador, P.; Dannenberg, J. J.; Zakrzewski, V. G.; Dapprich, S.; Daniels, A. D.; Strain, M. C.; Farkas, O.; Malick, D. K.; Rabuck, A. D.; Raghavachari, K.; Foresman, J. B.; Ortiz, J. V.; Cui, Q.; Baboul, A. G.; Clifford, S.; Cioslowski, J.; Stefanov, B. B.; Liu, G.; Liashenko, A.; Piskorz, P.; Komaromi, I.; Martin, R. L.; Fox, D. J.; Keith, T.; Al-Laham, M. A.; Peng, C. Y.; Nanayakkara, A.; Challacombe, M.; Gill, P. M. W.; Johnson, B.; Chen, W.; Wong, M. W.; Gonzalez, C.; Pople, J. A., Gaussian 09, revision B.09; Gaussian, Inc.: Pittsburgh, PA, 2009.

[38] http://www.biomolecular-modeling.com/Abalone.

[39] Watson, J. D.; Crick, F. H., Molecular structure of nucleic acids: A structure for deoxyribose nucleic acid. *Nature.* **1953**, *171*, 737-738. DOI: 10.1038/171737a0.

[40] Baker, E. S.; Bowers, M. T., B-DNA helix stability in a solvent-free environment. *J. Am. Soc. Mass. Spectrom.* **2007**, *18*, 1188-1195. DOI: 10.1016/j.jasms.2007.03.001.

[41] Jorgensen, W. L.; Chandrasekhar, J.; Madura, J. D.; Impey, R. W.; Klein, M. L., Comparison of simple potential functions for simulating liquid water. *J. Chem. Phys.* **1983**, *79*, 926-935. DOI: 10.1063/1.445869.

[42] Skyner, R. E.; McDonagh, J. L.; Groom, C. R.; van Mourik, T.; Mitchell, J. B. O., A review of methods for the calculation of solution free energies and the modelling of systems in solution. *Phys. Chem. Chem. Phys.* **2015**, *17*, 6174-6191. DOI: 10.1039/C5CP00288E.

[43] Essman, U.; Perera, L.; Berkowitz, M. L.; Darden, T.; Lee, H.; Pedersen, L. G., A smooth particle mesh Ewald method. *J. Chem. Phys.* **1995**, *103*, 8577-8593. DOI: 10.1063/1.470117.

[44] Wells, B. A.; Chaffee, A. L., Ewald summation for molecular simulations. *J. Chem. Theory Comput.* **2015**, *11*, 3684-3695. DOI: 10.1021/acs.jctc.5b00093.

[45] Darden, T.; York, D.; Pedersen, L., Particle mesh Ewald: An N-log(N) method for Ewald sums in large systems. *J. Chem. Phys.* **1993**, *98*, 10083-10092. DOI: 10.1063/1.464397.

[46] Uberuaga, B. P.; Anghel, M.; Voter, A. F., Synchronization of trajectories in canonical molecular-dynamics simulations:observation, explanation, and exploitation. *J. Chem. Phys.* **2004**, *120*, 6363-6374. DOI: 10.1063/1.1667473.

[47] Sindhikara, D. J.; Kim, S.; Voter, A. F.; Roitberg, A. E., Bad seeds sprout perilous dynamics: Stochastic thermostat induced trajectory synchronization in biomolecules. *J. Chem. Theory. Comput.* **2009**, *5*, 1624-1631. DOI: 10.1021/ct800573m.

[48] Miller III, B. R.; McGee Jr, T. D.; Swails, J. M.; Homeyer, N.; Gohlke, H,; Roitberg, A. E., MMPBSA.py: An efficient program for end-state free energy calculations. *J. Chem. Theory. Comput.* **2012**, *8*, 3314-3321. DOI: 10.1021/ct300418h.

[49] Gohlke, H.; Kiel, C.; Case, D. A., Insights into protein-protein binding by binding free energy calculation and free energy decomposition for the Ras-Raf and Ras-RalGDS complexes. *J. Mol. Biol.* **2003**, *330*, 891-913. DOI: 10.1016/S0022-2836(03)00610-7.

[50] Srinivasan, J.; Cheatham, T. E.; Cieplak, P.; Kollman, P. A.; Case, D. A., Continuum solvent studies of the stability of DNA, RNA, and phosphoramidate-DNA helices. *J. Am. Chem. Soc.* **1998**, *120*, 9401-9409. DOI: 10.1021/ja981844+.

[51] Wang, J.; Hou, T.; Xu, X., Recent advances in free energy calculations with a combination of molecular mechanics and continuum models. *Curr. Comput. Aided Drug Des.* **2006**, *2*, 287-306. DOI: 10.2174/157340906778226454.

[52] Wang, W.; Donini, O.; Reyes, C. M.; Kollman, P. A., Biomolecular simulations: Recent developments in force fields, simulations of enzyme catalysis, protein-ligand, protein-protein, and protein-nucleic acid noncovalent interactions. *Annu. Rev. Biophys. Biomol. Struct.* **2001**, *30*, 211-243. DOI: 10.1146/annurev.biophys.30.1.211.

[53] Daniel, R. R.; Cheatham III, T. E., PTRAJ and CPPTRAJ: Software for processing and analysis of molecular dynamics trajectory data. *J. Chem. Theor. Comput.* **2013**, *9*, 3084-3095. DOI: 10.1021/ct400341p.

[54] Kollman, P. A.; Massova, I.; Reyes, C.; Kuhn, B.; Huo, S. H.; Chong, L.; Lee, M.; Lee, T.; Duan, Y.; Wang, W.; Donini, O.; Cieplak, P.; Srinivasan, J.; Case, D. A.; Cheatham, T. E., Calculating structures and free energies of complex molecules: Combining molecular mechanics and continuum models. *Acc. Chem. Res.* **2000**, *33*, 889-897. DOI: 10.1021/ar000033j.

[55] Gohlke, H.; Case, D. A., Converging free energy estimates: MM-PB(GB)SA studies on the protein-protein complex Ras-Raf. *J. Comput. Chem.* **2004**, *25*, 238-250. DOI: 10.1002/jcc.10379.

[56] Young, M. A.; Ravishanker, G.; Beveridge, D. L., A 5-nanosecond molecular dynamics trajectory for B-DNA: analysis of structure, motions, and solvation. *J. Biophys.***1997**, *73*, 2313-2336. DOI: 10.1016/S0006-3495(97)78263-8.

[57] Coutsias, E. A.; Seok, C.; Dill, K. A., Using quaternions to calculate RMSD. *J. Comput. Chem.* **2004**, *25*, 1849-1857. DOI: 10.1002/jcc.20110.

[58] Genheden, S.; Ryde, U., The MM/PBSA and MM/GBSA methods to estimate ligand-binding affinities. *Expert Opin. Drug Discov.* **2015**, *10*, 449-461. DOI: 10.1517/17460441.2015.1032936.

[59] Genheden, S.; Ryde, U., How to obtain statistically converged MM/GBSA results. *J. Comput. Chem.* **2010**, *31*, 837-846. DOI: 10.1002/jcc.21366.

[60] Humphrey, W.; Dalk, A.; Schulten, K., VMD; Molecular Dynamic. *J. Molec. Graphics.* **1996**, *14*, 33-38. PMID: 8744570.

[61] Haris, P.; Mary, V.; Aparna, P.; Dileep, K. V.; Sudarsanakumar, C., A comprehensive approach to ascertain the binding mode of Curcumin with DNA. Spectrochim. *Acta Mol. Biomol. Spectrosc.* **2017**, *114*, 57-68. DOI: 10.1016/j.saa.2016.11.049.

[62] Yang, H.; Tang, P.; Tang, B.; Huang, Y.; He, J.; Li, S.; Li, H., Studies of DNA-binding properties of lafutidine as adjuvant anticanceragent to calf thymus DNA using multi-spectroscopic approaches, NMR relaxation data, molecular docking and dynamical simulation. *Int. J. Biol. Macromol.* **2017**, *99*, 79-87. DOI: 10.1016/j.ijbiomac.2017.02.062.

[63] Al-Otaibi, J. A.; Spittle, P. T.; EL Gogary, T. M., Interaction of anthraquinone anti-cancer drugs with DNA; Experimental and computational quantum chemical study. *J. Mol. Struct.* **1997**, *1127*, 751-760.

DOI: 10.1016/j.molstruc.2016.08.007.

[64] Morjani, H.; Tarantilis, P.; Polissiou, M.; Manfait, M., Growth inhibition and induction of crythroid differentiation activity by crocin, dimethylcrocetine and carotene on K562 tumor cells. *Anticancer Res.* **1990**, *10*, 1398-1406. PMID: 7847826.

[65] Brovarets, O. O.; Yurenko, Y. P.; Hovorun, D. M., The significant role of the intermolecular CH-O/N hydrogen bonds in governing the biologically important pairs of the DNA and RNA modified bases: a comprehensive theoretical investigation. *J. Biomol. Struct. and Dynam.* **2014**, *32*, 993-1022. DOI: 10.1080/07391102.2013.799439.

[66] Brovarets, O. O.; Yurenko, Y. P.; Hovorun, D. M., Intermolecular CH…O/N H-bonds in the biologically important pairs of natural nucleobases: a thorough quantum-chemical study. *J. Biomol. Struct. and Dynam.* **2015**, *33*, 1624-1652. DOI: 10.1080/07391102.2014.968623.